

Energy-Efficient Power Allocation with Individual and Sum Power Constraints

Peter He, *Member, IEEE*, Shan Zhang, *Member, IEEE*,
Lian Zhao, *Senior Member, IEEE*, and Xuemin (Sherman) Shen, *Fellow, IEEE*.

Abstract—In this paper, we investigate the power allocation in a multi-user wireless system to maximize the Energy efficiency (EE), while meeting the power constraints of each individual user as well as the whole system. Specifically, a geometric ceiled-water-filling algorithm is proposed to solve this non-linear fractional optimization problem, which can compute exact solutions with a low degree of polynomial computational complexity. Optimality of the proposed algorithm is strictly proved with mathematic analysis. In addition, the proposed algorithm is further extended to the general case with the minimum system-level throughput constraint, considering the quality of service (QoS) requirement. To the best of our knowledge, no prior algorithm in the open literature offered such optimal solutions to the target problems, with the merit of exactness and the efficiency. Simulation results demonstrate that the proposed power allocation algorithms can improve the energy efficiency by nearly 50%, compared with the conventional Dinkelbach’s method with the same amount of computations.

Keywords

Energy efficiency (EE), exactness, Geometric Water-Filling (GWF), non-linear fractional optimization, polynomial computational complexity, power allocation.

I. INTRODUCTION

Green communication technologies are considered as cornerstones to achieve sustainable network development and operations, which is the key to reduce operational expenditure as well as prolong the life of battery powered Internet of Things (IoT) devices [1], [2]. Accordingly, how to improve energy efficiency, *i.e.*, the ratio of throughput to energy consumption [3], [4], has become a critical design objective in the future wireless networks [5], [6]. Extensive works have been conducted on green communications [7], [8], where the fundamental problems can be classified into three categories: (1) throughput maximization with power constraints [9]–[11]; (2) power minimization with throughput requirements [12]–[16]; and (3) Energy Efficiency (EE) maximization with/out power and throughput constraints [17]. The EE maximization problem, generally

formulated as a non-linear fractional optimization problem, is the most challenging one, where the Karush-Kuhn-Tucker (KKT) conditions usually present complicated structure and cannot be solved directly [18]–[20].

In the existing literature, iterative algorithms are applied to address the EE maximization problems [21]–[26], and Dinkelbach’s method has been widely adopted. In [21], a combinatorial optimization problem has been formulated to maximize the energy efficiency of both transmitter and receiver with the minimum throughput requirement, where a novel divide-and-conquer approach is proposed to find a sub-optimal solution [21, p. 2728]. [23] investigated the energy-efficient resource allocation problem in an OFDM downlink system, where an algorithm is proposed based on a transformation of Dinkelbach’s method. Although insightful, the existing methods are either sub-optimal or require high complexity.

Different from the existing works, this paper firstly proposes a geometric ceiled-water-filling (GC-WF) algorithm to directly obtain the optimal solution to the EE maximization problem with power constraints of both system and individual users, by exploiting the water-filling structure of optimal solutions. A wireless communication system with multiple parallel users is considered, where each user can be a IoT device (*i.e.*, data collecting and monitoring system) or a channel of the massive MIMO system. Each individual user has peak power constraints depending on the battery status and field requirements (such as reducing interference, avoiding power saturation and out-of-band power leakage), while the sum power of the whole system is also constrained considering the operational costs. In fact, the studied problem regresses to the conventional EE maximization problem without individual peak power constraints, when the individual peak power constraints are relaxed (*i.e.*, the value of peak power are sufficiently large). Accordingly, the EE maximization problem with individual power constraints is more general as well as more practical. However, with the individual peak power constraints, the set of feasible power allocation presents more complicated structure, bringing new challenges to problem analysis. To address the challenges, a multi-channel water tank illustration with ceilings is utilized to illustrate the power allocation process analysis, where the ceilings depict the individual peak power constraints in a geometric way. Then, a geometric ceiled-water-filling (GC-WF) algorithm is proposed, which can provide the optimal solution with low degree of polynomial

Peter He and Xuemin (Sherman) Shen are with the Department of Electrical and Computer Engineering, University of Waterloo, 200 University Avenue West, Waterloo, Ontario, Canada, N2L 3G1 (Email: {z85he, sshen}@uwaterloo.ca).

Shan Zhang (corresponding author) is with Beijing Key Laboratory of Computer Networks, the School of Computer Science and Engineering, Beihang University, Beijing, 100191, P.R.China. (Email: zhangshan18@buaa.edu.cn).

Lian Zhao is with Dept. of Electrical and Computer Engineering, Ryerson University, Ontario, Canada, M5B 2K3. (E-mail: l5zhao@ryerson.ca).

computational complexity. The insights are that the EE-optimal power allocation satisfies the geometric water-filling like architecture, whereas the water levels of different channels further depend on the individual peak power requirements. Furthermore, the GC-WF algorithm is extended to solve the more generalized EE optimization problems with a minimum throughput requirement added. As the side notes, algorithms proposed by this paper, utilize the algorithms of [27] and [12] for preparation. The algorithms of [27] and [12] aimed to solve the two different classes of the problems on throughput optimization and power minimization, respectively. Instead, this paper solves the third class of the problems on energy efficiency maximization, considering both individual and system power constraints. Although [17] also solved the energy efficiency maximization problems with the sum power constraints, it cannot apply to the systems with individual power constraints.

The advantages of the proposed algorithm are two-fold, *exactness and efficiency*, which can not be simultaneously guaranteed by existing works according to the authors' knowledge. *Exactness* means that the proposed algorithm can output the computational results with machine-zero error compared with the "theoretic" optimal ones, *i.e.*, no larger than 10^{-34} based on the standard of IEEE 754-2008. In addition, the proposed algorithm is of high efficiency, which can output the solutions with a low degree polynomial computational complexity. Exactness of the proposed algorithm is proved with strict mathematical analysis, and the low complexity is analyzed as well as validated through numerical results. With these two-folds benefits, the proposed algorithm can be applied to sustainable and efficient power management in large-scale wireless communication systems, such as IoT-based big data collection and smart city monitoring.

The remainder of this paper is organized as follows. As preparation, Section II reviews the geometric water-filling algorithm to solve two simple but fundamental power allocation problems with individual peak power constraints: (1) throughput optimization, and (2) sum power minimization. In Section III, the ceiled water tank illustration is firstly proposed, based on which we develop the GC-WF algorithm to solve the EE maximization problem with sum and individual peak power constraints. In addition, the proposed GC-WF algorithm is extended in Section IV to solve the more general EE maximization problem with an additional minimum throughput requirement, named as GC-WFT. Then, the proposed algorithm is also compared with the conventional Dinkelbach's method theoretically for better understanding. Section V presents numerical examples and complexity analysis to illustrate the procedures of the proposed algorithms and the efficiency. Finally, Section VI concludes the paper.

II. GEOMETRIC WATER-FILLING ALGORITHM REVIEW

In this section, we review geometric water-filling (GWF) algorithm to solve the throughput maximization and power

minimization problems with individual peak power constraints, *i.e.*, GWFPP [27] and P-GWFPP [12], respectively. These algorithms are reviewed as preparation to solve the EE maximization problem, with further development introduced in the following sections.

Consider a wireless communication system with K channels¹, where the power gain of the k th channel is given by a_k for $k = 1, 2, \dots, K$. Denote by P the power budget of the whole system, P_k the peak power constraint of the k th channel, $s_0 > 0$ the constant circuit power, and s_k the power allocated to the k th channel. For generality, each channel has a weight factor that takes a positive numerical value, denoted as w_k for $k = 1, 2, \dots, K$, to represent the different level of importance. Then, the power allocation problem is to find a group of power $\{s_k\}$ to optimize the specific objectives, *eg.*, throughput maximization, power minimization, and EE maximization. Without loss of generality, assume $\{a_k w_k\}_{k=1, \dots, K}$ is a sorted sequence with strictly monotonically decreasing in k (the indexes can be arbitrarily renumbered to satisfy this condition) for analysis.

A. Throughput maximization with Algorithm GWFPP

Denote by E_0 the set of channels considered for power allocation, which is a subset of $\{1, \dots, K\}$ ². The throughput-optimal power allocation can be formulated as follows.

$$\begin{aligned} \max_{\{s_i\}_{i \in E_0}} & \frac{1}{2} \sum_{i \in E_0} w_i \log_2(1 + a_i s_i) \\ \text{(GWFPP)} \quad \text{s.t.} & \quad 0 \leq s_i \leq P_i, \quad i \in E_0; \\ & \quad \sum_{i \in E_0} s_i \leq P. \end{aligned} \quad (1)$$

Applying water-filling method, the *depth* of the k th stair is the height of the k th step to the bottom of the tank [27], denoted by

$$d_k = \frac{1}{a_k w_k}, \quad k \in E_0. \quad (2)$$

GWF first determines the index, k^* , the highest step under water:

$$k^* = \max \left\{ k \mid \hat{P}(k) > 0, \quad k \in E_0 \right\}, \quad (3)$$

where $\hat{P}(k)$ is a function in k , denoting the water volume above the k th step. From the geometric relationship, $\hat{P}(k)$ can be obtained by

$$\hat{P}(k) = \left[P - \sum_{i \in \{1 \leq i \leq k-1\}} w_i \left(\frac{1}{a_k w_k} - \frac{1}{a_i w_i} \right) \right]^+, \quad (4)$$

for $k \in E_0$, where $[x]^+ = \max\{x, 0\}$, a piecewise linear function. Then, the power allocated for the k^* th channel is

$$s_{k^*} = \frac{w_{k^*}}{\sum_{i \in \{1 \leq i \leq k^*\} \cap E_0} w_i} \hat{P}(k^*), \quad (5)$$

and the completed solution is

$$s_i = \begin{cases} \left[\frac{s_{k^*}}{w_{k^*}} + \left(\frac{1}{a_{k^*} w_{k^*}} - \frac{1}{a_i w_i} \right) \right] w_i & \{1 \leq i \leq k^*\} \cap E_0; \\ 0, & \{k^* < i\} \cap E_0. \end{cases} \quad (6)$$

¹The problems and algorithms in this paper are all based on this system, where "channels" and "users" are used alternately with one-to-one mapping.

²Noting the fact that any set is a subset of itself

Algorithm GWFP is listed as follows.

Algorithm GWFP:

Input: vector $\{d_i = \frac{1}{a_i w_i}\}, \{w_i\}, \{P_i\}$ for $i = 1, 2, \dots, K$, the set $E_0 = \{1, 2, \dots, K\}$, and P .

- 1) Utilize (3)-(6) to compute $\{s_i\}$.
- 2) The set Λ is defined by the set $\{i | s_i > P_i, i \in E_0\}$. If Λ is the empty set, output $\{s_i\}_{i=1}^K$ and $E_f = E_0$; else, $s_i = P_i$, as $i \in \Lambda$.
- 3) Update E_0 with $E_0 \setminus \Lambda$ and P with $P - \sum_{t \in \Lambda} P_t$, and return to Step 1).

Remark 1. Algorithm GWFP carries out at most K loops to compute the optimal solution, with computational complexity of $O(K^2)$. We use $\text{GWFP}(\{a_i, w_i, P_i\}_{i=1}^K, P)$ to represent the mapping from $\{\{a_i, w_i, P_i\}_{i=1}^K, P\}$ to $\{E_f, k^*, \hat{P}(k^*)\}$ through Algorithm GWFP, where E_f is the set of channels allocated with power below their peak requirements.

B. Power minimization with Algorithm P-GWFP

The power minimization problem is formulated as follows:

$$\begin{aligned} \min_{\{s_i\}_{i=1}^K} \quad & \sum_{i=1}^K s_i \\ \text{(P-GWFP)} \quad & \text{s.t. } 0 \leq s_i \leq P_i, \text{ for } i = 1, \dots, K; \\ & \frac{1}{2} \sum_{i=1}^K w_i \log(1 + a_i s_i) \geq B, \end{aligned} \quad (7)$$

and [12] has provided the solution without the individual peak power constraints:

$$k^* = \max \left\{ k \mid ER(k) < \eta (= 2^{2B}), 1 \leq k \leq K \right\}, \quad (8)$$

with $ER(k)$ defined by:

$$ER(k) = \prod_{i=1}^{k-1} \left(\frac{a_i w_i}{a_k w_k} \right)^{w_i}, \text{ for } k = 1, \dots, K. \quad (9)$$

The power level for this step is

$$s_{k^*} = \frac{1}{a_{k^*}} \left[\left(\frac{\eta}{ER(k^*)} \right)^{\frac{1}{\sum_{i=1}^{k^*} w_i}} - 1 \right]. \quad (10)$$

Then, the power allocation for the i th channel is given by

$$s_i = \begin{cases} \left[\frac{s_{k^*}}{w_{k^*}} + \left(\frac{1}{a_{k^*} w_{k^*}} - \frac{1}{a_i w_i} \right) \right] w_i, & 1 \leq i \leq k^*; \\ 0, & k^* < i. \end{cases} \quad (11)$$

If the obtained power allocation satisfies the individual peak power constraints, it is the optimal solution to (P-GWFP). Otherwise, the channels with power overflow should be allocated with their peak power and removed out of the system, and the power allocation to the other channels should be resolved, until all channels meet the individual peak power constraints. Algorithm P-GWFP is stated as follows.

Algorithm P-GWFP:

Input: arrays $\{a_i, w_i, P_i\}$ for $i = 1, 2, \dots, K$, the set $E_0 = \{1, 2, \dots, K\}$, and $\eta = 2^{2B}$.

- 1) Utilize (8)-(10), and (6) to compute $\{s_i\}$.
- 2) The set Λ is defined by the set $\{i | s_i > P_i, i \in E_0\}$. If Λ is the empty set, output $\{s_i\}_{i=1}^K$; else, $s_i = P_i$, for $i \in \Lambda$.
- 3) Update E_0 with $E_0 \setminus \Lambda$ and η with $\eta / [\prod_{t \in \Lambda} (1 + a_t P_t)^{w_t}]$, and return to Step 1).

Remark 2. Algorithm P-GWFP carries out at most K loops to obtain the optimal solution, with the computational complexity of $O(K^2)$. Algorithm P-GWFP provides the mapping from $\{\{a_i, w_i, P_i\}_{i=1}^K, B\}$ to the exact solution of Problem (P-GWFP), $\{s_i\}, k^*$ and $E_{p,f}$, where $E_{p,f}$ denotes the finally obtained index set.

III. PROBLEM STATEMENT AND PROPOSED GC-WF ALGORITHM

In this section, we first formulate the EE maximization problem with sum and individual peak power constraints, and introduce the ceiled water tank illustration to the problem. We then propose the GC-WF algorithm to solve the EE maximization problem.

A. Problem Statement

The EE-optimal power allocation problem can be formed as follows:

$$\begin{aligned} \max_{\{s_k\}_{k=1}^K} \quad & \frac{\frac{1}{2} \sum_{k=1}^K w_k \log_2(1 + a_k s_k)}{s_0 + \sum_{k=1}^K s_k} \\ \text{(EE-SI)} \quad & \text{s.t. } 0 \leq s_k \leq P_k, \text{ for } k = 1, \dots, K; \\ & \sum_{k=1}^K s_k \leq P, \end{aligned} \quad (12)$$

where the objective function is the weighted energy efficiency, the first constraint comes from individual peak power constraints, and the second constraint corresponds to the total power budget. The (EE-SI) problem has a non-linear fractional objective function.

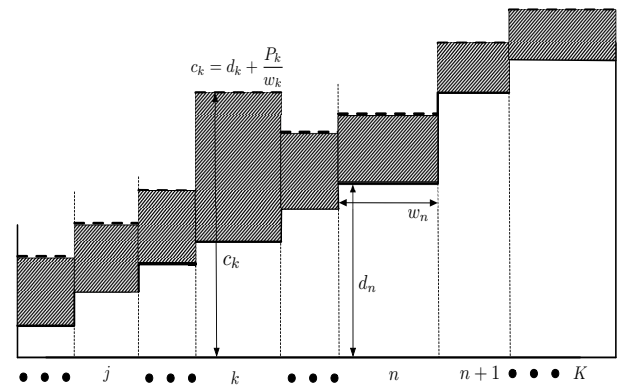


Fig. 1: Ceiled water tank illustration.

B. Ceiled Water Tank Illustration

Without losing generality, suppose that $\{a_k w_k\}_{k=1}^K$ are sorted with strictly monotonically decreasing in k . We introduce a ceiled water tank illustration to describe the geometric relationship of the communication system,

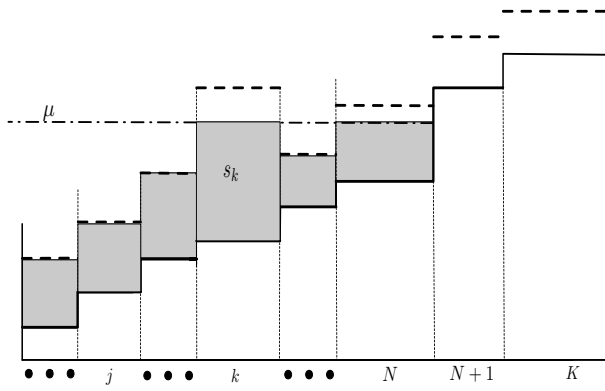


Fig. 2: An illustration of power allocation with water level μ .

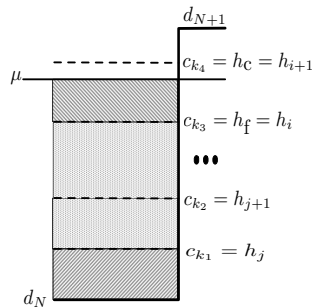


Fig. 3: Ceilings located in the interval of $[d_N, d_{N+1}]$.

illustrated as Fig. 1. The K stairs correspond to the K channels. For the k th stair, the width equals the weight factor w_k , and the height d_k is set as $d_k = \frac{1}{a_k w_k}$. The bold dashed line segments over the specific steps depict the peak power constraints for the corresponding channels, which are referred to as *ceilings* in this paper, given by

$$c_k = d_k + \frac{P_k}{w_k} \quad (13)$$

for the k th channel. Correspondingly, the height of each stair, $\{d_k\}$, is named as *floors* for better understanding. With this water tank illustration, the power allocated to the k th channel equals the area of water above the floor of the k th stair. Notice that the width of each stair reflects the importance of the channel, and channels with larger width are expected to obtain more power. In addition, the height of each stair reflects the channel condition, and stairs with higher floors indicates deeper channel fading, which are expected to obtain less power. Furthermore, the ceilings reflect the maximum amount of water allocated to each stair, which further constrains the maximum power allocation. Thus, the shaded area shown in Fig. 1 is called the feasible region of power allocation in this paper.

The EE-optimal power allocation problem without individual power constraints has been investigated in our previous work [17], where a similar water tank illustration is applied but without ceilings. In that case, the feasible region of power allocation is entire area above the stair floors. After determining the optimal water level, the power

allocated to each channel can be obtained. In this paper, the power allocated to each channel further depends on the corresponding ceilings in addition to the water level, and the existing method does not apply.

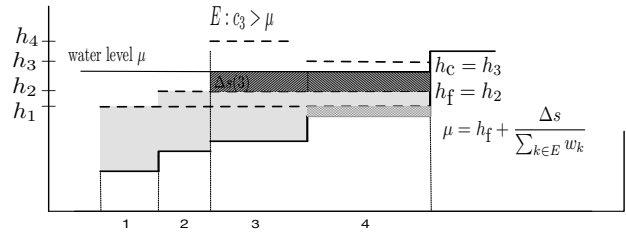


Fig. 4: Sorted sequence $\{h_j\}$, and power allocated inside the tunnel of Δs ($N = 4$; $j = 1, 2$ and $k = 3, 4$).

Fig. 2 illustrates the influences of water level and ceilings on the power allocation. When a certain amount of power is poured into the tank, suppose the water level μ is between the N th and $(N + 1)$ th stairs, as illustrated in Fig. 2. The K channels are classified into three groups:

- i) The power allocated is constrained by the peak power, for example, $c_j \leq \mu$ and thus $s_j = P_j$ for the j th channel;
- ii) The power allocated is less than the peak constraint, for example, $c_k > \mu$ and thus $s_k = w_k(\mu - d_k)$ for the k th channel;
- iii) No power is allocated due to bad channel condition, for example, $\mu \leq d_{N+1}$ for the $(N + 1)$ th channel.

Therefore, the ceilings bring significant challenges to the power allocation problem. To deal with this challenge, preprocessing is conducted with respect to the ceilings, based on which we propose the algorithm to solve the (EE-SI) problem.

C. Preprocessing of Ceilings

Assume that a certain amount of power is poured into the water tank and the corresponding water level μ is between the N th and the $(N + 1)$ th steps, as shown in Fig. 3. For channel N , the ceiling in the interval of d_1 to d_{N+1} can influence the results of water level and corresponding power allocation, and we conduct preprocessing of these ceilings before determining the power level. Firstly, the ceilings within interval $[d_1, d_{N+1}]$ form a set:

$$\{c_k | d_1 < c_k < d_{N+1}, 1 \leq k < N + 1\}. \quad (14)$$

Denote by $\tilde{K}_c = |\{c_k | d_1 < c_k < d_{N+1}, 1 \leq k < N + 1\}|$, the number of ceilings falling into interval $[d_1, d_{N+1}]$. Sort these ceilings into a monotonically increasing sequence

$$\{h_j\}_{j=1}^{\tilde{K}_c}, \quad (15)$$

through the mapping σ of a permutation from the index set of the c_k sequence to that of the h_k sequence. As a side note of

Fig. 3, the subscript sequence $\{k_1, \dots, k_4\}$ of $\{c_{k_1}, \dots, c_{k_4}\}$ are the subset of $\{1, 2, \dots, \hat{K}_c\}$, which may not be $\{1, \dots, 4\}$.

Denote by K_c the number of ceilings falling into the interval (d_N, d_{N+1}) . There are three cases:

- i) $K_c > 1$, multiple ceilings falling into the interval;
- ii) $K_c = 1$, just one ceiling falling into the interval;
- iii) $K_c = 0$, no ceiling falling into the interval.

Fig. 3 is an illustration of the first case, where $\hat{K}_c \geq K_c \geq 4$. With the ceilings sorted into $\{h_i\}_{i=1}^{\hat{K}_c}$, the interval (d_N, d_{N+1}) is further divided into $K_c + 1$ subintervals. Suppose the water level falls into the i th subinterval without loss of generality, i.e., $h_i \leq \mu < h_{i+1}$, shown as Fig. 3. We define the term ‘‘tunnel’’, referring to the i th subinterval $[h_i, h_{i+1}]$. We also use ‘‘tunnel floor ($h_f = h_i$)’’ and ‘‘tunnel ceiling ($h_c = h_{i+1}$)’’ respectively to denote the two closet ceilings to the water level μ . For better understanding on the preprocessing of ceilings, Fig. 4 illustrates the sorted sequence $\{h_j\}$, as shown in the left most vertical axis. The ceilings of four channels are sorted into $\{h_1, h_2, h_3, h_4\}$, and ceilings $\{h_1, h_2, h_3\}$ fall into the interval $[d_4, d_5]$ (when considering $N = 4$). When the water level further falls in subinterval $[h_2, h_3]$, h_2 and h_3 serve as tunnel floor and tunnel ceiling, respectively.

The allocated power for the N th step, $s_N = w_N(\mu - d_N)$, can be described as the sum of the stripped areas shown in Fig. 3,

$$s_N = w_N[(\mu - h_f) + \sum_{j \in \{j|h_f > h_j > d_N\}} (h_{j+1} - h_j) + (h_{\min\{j|h_j > d_N\}} - d_N)], \quad (16)$$

where the three terms correspond to the three areas with different shadows, respectively.

D. Power Allocation within Tunnel

For notation simplicity, the additional power allocated to a channel when the water level rises from the tunnel floor to μ ($h_f \leq \mu < h_c$) is referred to as power allocation within tunnel. Denote by $\Delta s(k)$ the power allocation within tunnel for the k th channel, for $k = 1, 2, \dots, N$. For example, the power allocation within tunnel for the N th channel is given by

$$\Delta s(N) = w_N(\mu - h_f), \quad (17)$$

shown as the slashed line shaded area above the N th stair in Fig 4. Notice that channels $\{1, 2, \dots, N-1\}$ can be classified into two groups based on their allocated power within tunnel. If the channel ceiling is lower than the tunnel floor, no power is allocated for this channel within tunnel, for example, $\Delta s(j) = 0$ for the j th channel in Fig. 4. Otherwise, additional power is allocated, for example, the power $\Delta s(k) = w_k(\mu - h_f)$, shown as the slashed shaded area over the k th stair in Fig. 4. Denote by E the second group of channels, $E = \{k|h_{\sigma(k)} > h_f, 1 \leq k \leq N\}$, and E^c the first group of channels, $E^c = \{k|h_{\sigma(k)} \leq h_f, 1 \leq k \leq N\}$ ³. Thus, the set E includes the channels

³For the special case $N = 1$, the set E can be defined as a singleton, $\{1\}$, and the E^c would be defined as the empty set of \emptyset .

of positive power allocations within tunnel, i.e., $\{\Delta s(k) > 0|k \in E\}$. According to Fig. 4, the total power within tunnel allocated to all channels is given by

$$\Delta s = \sum_{k \in E} \Delta s(k), \quad (18)$$

shown as the total slashed shaded areas in Fig. 4. Applying the concepts of the tunnel floor h_f , power within tunnel Δs , and the set E , the water level is expressed as

$$\mu = h_f + \frac{\Delta s}{\sum_{k \in E} w_k}. \quad (19)$$

From the geometric relationship illustrated by Fig. 4, Δs has a domain $[\Delta s_{\min}, \Delta s_{\max}]$, where

$$\begin{cases} \Delta s_{\min} &= 0; \\ \Delta s_{\max} &= (h_c - h_f) \sum_{k \in E} w_k. \end{cases} \quad (20)$$

As a reminder, Fig. 4 has assigned $N = 4, j = 1, 2$ and $k = 3, 4$, as an instance for conveniently understanding. Here Δs_{\max} is obtained at the highest water level $\mu = h_c$ in the tunnel, i.e., the tunnel is fully loaded. If more water is poured in the system, the water level will fall into the next subinterval $[h_{i+1}, h_{i+2}]$, and a new tunnel will form. As a side note, Δs_{\max} may also be written as $\Delta s_{\max}(i, N)$, to emphasize its dependence on the indexes of i and N , i.e., the i th ceiling h_i serving as the tunnel floor in the interval of $[d_N, d_{N+1}]$.

E. EE-Optimal Power Allocation within A Tunnel

To determine the optimal water level and power allocation within the tunnel $[h_f, h_c] = [h_i, h_{i+1}]$, we firstly introduce a function $g(\Delta s)$

$$g(\Delta s) = \left(h_f + \frac{\Delta s}{\sum_{k \in E} w_k} \right) \cdot \left\{ \sum_{k \in E} w_k \left[\log \left(h_f + \frac{\Delta s}{\sum_{k \in E} w_k} \right) - \log(d_k) \right] + \sum_{j \in E^c} w_j \log \left(\frac{h_{\sigma(j)}}{d_j} \right) \right\} - \left[s_o + \sum_{k \in E} s_k + \sum_{j \in E^c} w_j (h_{\sigma(j)} - d_j) \right]. \quad (21)$$

The objective function of problem (12) has fractional form, and function $g(\Delta s)$ is related to the gradient of the numerator. Thus, $g(\Delta s)$ can reflect the optimality of objective function. The detailed derivation of $g(\Delta s)$ is omitted due to the page limit. Then, the power allocated to the k th channel ($k \in E$) can be expressed as

$$s_k = \left[(h_f - d_k) + \frac{\Delta s}{\sum_{k \in E} w_k} \right] w_k, \forall k \in E. \quad (22)$$

Using the concept of water level μ , with the notation $\mu_j = h_{\sigma(j)}$ at $j \in E^c$, $g(\Delta s)$ is expressed with a clear geometric meaning of the parameters:

$$g(\Delta s) = \mu \left[\sum_{k \in E} w_k \log \left(\frac{\mu}{d_k} \right) + \sum_{j \in E^c} w_j \log \left(\frac{\mu_j}{d_j} \right) \right] - \left[s_o + \sum_{k \in E} w_k (\mu - d_k) + \sum_{j \in E^c} w_j (\mu_j - d_j) \right]. \quad (23)$$

For a given tunnel, consider an optimization problem in terms of Δs

$$\begin{aligned} & \min_{\Delta s} |g(\Delta s)|, \\ \text{s.t. } & 0 \leq \Delta s \leq \Delta s_{\max}(i, N), \end{aligned} \quad (24)$$

whose optimal solution provides the optimal water level of the EE-optimal power allocation within tunnel $[h_i, h_{i+1}]$. Proposition 1 provides the optimal solution to (24).

Proposition 1. For any given i and N involved in forming problem (24), the solution to this system is computed by three cases: if $g(0) < 0$ and $g(\Delta s_{\max}) > 0$, the solution can be computed from the following iteration,

$$\Delta s_{n+1} = \Delta s_n - \frac{g(\Delta s_n)}{g'(\Delta s_n)}, \forall n \in \mathbb{Z}^+, \quad (25)$$

where \mathbb{Z}^+ is the set of non-negative integers and the subscript of Δs_n is the iteration index; if $g(0) \geq 0$, the solution is $\Delta s = 0$; else if $g(\Delta s_{\max}) \leq 0$, the solution is $\Delta s = \Delta s_{\max}$. In addition, no case of $g(0) > 0$ and $g(\Delta s_{\max}) < 0$ exists.

Proof. See Appendix A. \square

Remark 3. Proposition 1 computes the optimal power allocation when the power level is within the specific tunnel. For the first case, Proposition 1 needs N_t (derived in Appendix A) loop operations, to compute the exact solution to the problem (24) at most, which shows low polynomial computational complexity with respect to system parameters. Proposition 1 is regarded as the mapping of $(s_0, N, \{d_k\}_{k=1}^K, [h_f, h_c])$ to the exact solution of power level within tunnel. Problem (24) can be regarded as a transform of EE-optimal power allocation, which is solvable with low complexity and provides the basis for EE-optimal power allocation algorithm design. The underlying rationale is that the EE-optimal solutions also own the water-filling architecture.

F. Proposed Algorithm GC-WF

Based on the concept of power ceilings, tunnels, Proposition 1, and GWFP algorithm, we propose Algorithm GC-WF to solve the target problem (EE-SI) as follows.

Algorithm GC-WF:

0) Initialization:

$$\begin{aligned} & \{E_f, k^*, \hat{P}(k^*)\} \\ & = \text{GWFP} \left(\{a_k, w_k, P_k\}_{k=1}^K, \min \left\{ \sum_{k=1}^K P_k, P \right\} \right) \\ & \text{and} \\ & a_{K+1} w_{K+1} = \left(\frac{\hat{P}(k^*)}{\sum_{k \in E} w_k} + \frac{1}{a_{k^*} w_{k^*}} \right)^{-1}. \end{aligned} \quad (26)$$

1) Input:

$$s_0, \{a_k, w_k\}_{k=1}^K, a_{K+1} w_{K+1}, N = 1 \text{ and assigning a } K \times K \text{ matrix } \mathbf{S} \text{ a null matrix.}$$

2) Loop for N from 1 to K : for each loop, one of the following three branches being implemented to update the N th row of the matrix \mathbf{S} :

2.1) If there is no ceiling falling in the interval (d_N, d_{N+1}) , the tunnel floor and ceiling are assigned by d_N and d_{N+1} respectively, expressed as

$$\{c_k | d_N < c_k < d_{N+1}, 1 \leq k \leq N\} = \emptyset, \quad (27)$$

$$[d_N, d_{N+1}] \rightarrow [h_f, h_c] \text{ in Proposition 1.}$$

⁴ Based on $g(\Delta s)$ defined by (23) and Proposition 1, we have three sub-branches:

2.1.1) If $g(0) > 0$, then $h_f = d_N$ and $h_c = d_{N+1}$ (see Fig. 5(a)), the power allocation is

$$\begin{cases} S_{N,k} = (d_N - d_k)w_k, & k \in E; \\ S_{N,j} = P_j, & j \in E^c. \end{cases}$$

Then go to Step 3); else

2.1.2) if

$$g(\Delta s_{\max}) = g((d_{N+1} - d_N) \sum_{k \in E} w_k) < 0,$$

then $h_f = d_N, h_c = d_{N+1}$ (see Fig. 5(b)), the power allocation is

$$\begin{cases} S_{N,k} = (d_{N+1} - d_k)w_k, & k \in E; \\ S_{N,j} = P_j, & j \in E^c. \end{cases}$$

Then go to Step 3); else

2.1.3) if

$$g(0) \cdot g((d_{N+1} - d_N) \sum_{k \in E} w_k) < 0,$$

then $h_f = d_N, h_c = d_{N+1}$ (see Fig. 5(c)), tunnel total power Δs is solved by (25) in Proposition 1, and

$$\begin{cases} S_{N,k} = \left[\frac{\Delta s}{\sum_{k \in E} w_k} + (d_N - d_k) \right] w_k, & k \in E; \\ S_{N,j} = P_j, & j \in E^c. \end{cases}$$

Then go to Step 3).

2.2) If there are one or more ceilings in the interval $[d_N, d_{N+1}]$ (i.e., $K_c \geq 1$), denote by $\mathcal{I}_N = K_c + 1$ the number of subintervals. We form a new sequence $\{\bar{h}_k\}_{k=0}^{\mathcal{I}_N}$ as

$$\{d_N, d_{N+1}\} \cup \{c_k | d_N < c_k < d_{N+1}, 1 \leq k \leq N\}$$

where

$$d_N = \bar{h}_0 < \bar{h}_1 < \dots < \bar{h}_{\mathcal{I}_N} = d_{N+1} \quad (28)$$

Assign an $\mathcal{I}_N \times K$ matrix $\bar{\mathbf{S}}$ a null matrix. Then, loop for t from 1 to \mathcal{I}_N in step 2.3): for each loop, one of the following three branches being implemented to update the t th row of $\bar{\mathbf{S}}$.

2.3) Assign \bar{h}_{t-1} and \bar{h}_t to tunnel floor and ceiling, respectively, and update the $g(\Delta s)$.

2.3.1) If $g(0) > 0$,

$$\begin{cases} \bar{S}_{N,k} = (\bar{h}_{t-1} - d_k)w_k, & k \in E; \\ \bar{S}_{N,j} = P_j, & j \in E^c. \end{cases}$$

Then go to Step 2.3.4); else

⁴In the expression above, “ \rightarrow ” denotes the assignment operation.

2.3.2) if

$$g\left(\left(\bar{h}_t - \bar{h}_{t-1}\right) \sum_{k \in E} w_k\right) < 0,$$

$$\begin{cases} \bar{S}_{N,k} = (\bar{h}_t - d_k)w_k, & k \in E; \\ \bar{S}_{N,j} = P_j, & j \in E^c. \end{cases}$$

Then go to Step 2.3.4); else

2.3.3) if

$$g(0) \cdot g\left(\left(\bar{h}_t - \bar{h}_{t-1}\right) \sum_{k \in E} w_k\right) < 0,$$

Then Δs can be solved by applying (25). And

$$\begin{cases} \bar{S}_{N,k} = \left[\frac{\Delta s}{\sum_{k \in E} w_k} + (\bar{h}_{t-1} - d_k) \right] w_k, & k \in E; \\ \bar{S}_{N,j} = P_j, & j \in E^c. \end{cases}$$

Then go to Step 2.3.4).

2.3.4) If $t = \mathcal{I}_N$, compute

$$t^* = \arg \max_{\{t | 1 \leq t \leq \mathcal{I}_N\}} \left\{ \frac{\frac{1}{2} \sum_{k=1}^K w_k \log_2(1+a_k \bar{S}_{N,k})}{s_0 + \sum_{k=1}^K \bar{S}_{N,k}} \right\}, \quad (29)$$

output $S_{N,k} = \bar{S}_{t^*,k}, \forall k$, and then go to Step 3); else let $t+1 \rightarrow t$ and go to Step 2.3).

3) If $N = K$, compute

$$n^* = \arg \max_{\{N | 1 \leq N \leq K\}} \left\{ \frac{\frac{1}{2} \sum_{k=1}^K w_k \log_2(1+a_k S_{N,k})}{s_0 + \sum_{k=1}^K S_{N,k}} \right\}, \quad (30)$$

and then output $\bar{s}_k = S_{n^*,k}, \forall k$; else let $N+1 \rightarrow N$ and go to Step 2.1).

To help understand the algorithm, Step 2.1 and Step 2.2 are illustrated by Fig. 5 and Fig. 6 respectively.

Proposition 2. GC-WF outputs the solution to the problem in (12), with a finite amount of computation.

Proof. See Appendix B. \square

For the complexity analysis of Algorithm GC-WF, we have the following corollary.

Corollary 1. In Algorithm GC-WF, the iterative computation of Eq. (25) in Proposition 1 is required once at most.

Proof. Let $h_f^{(i)}$ and $h_c^{(i)}$ denote the floor and ceiling of the i th tunnel respectively. Within the i th tunnel, we have $[h_f^{(i)}, h_c^{(i)}] \subset [d_1, d_{N+1}]$. It has been proved that $g(\Delta s)$ is monotonically increasing, according to the first paragraph in the proof of Proposition 1. It is seen that for a larger interval $[d_1, d_{m+1}]$, where $m > N$, this larger interval still includes the given $[h_f^{(i)}, h_c^{(i)}]$. At the same time, let V_i^{\min} and V_i^{\max} denote the minimum and the maximum values of $g(\Delta s(\mu))$ over $[h_f^{(i)}, h_c^{(i)}]$, then

$$\begin{aligned} V_i^{\min} &= g\left(\Delta s(\mu = h_f^{(i)})\right) = g(\Delta s = 0) \\ V_i^{\max} &= g\left(\Delta s(\mu = h_c^{(i)})\right) \\ &= g\left(\Delta s = \left(h_c^{(i)} - h_f^{(i)}\right) \cdot \sum_{k \in \{k | h_{\sigma(k)} > h_f^{(i)}, 1 \leq k \leq N\}} w_k\right), \end{aligned}$$

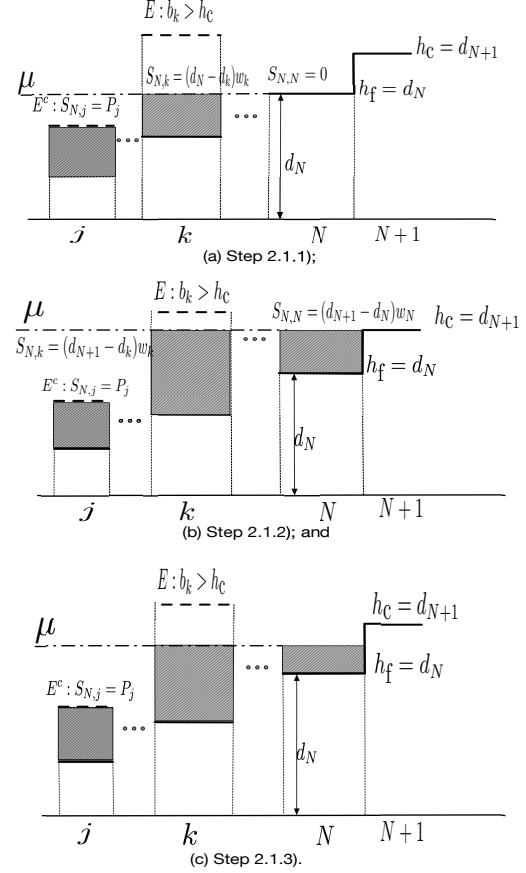


Fig. 5: Illustration of Step 2.1 of Algorithm GC-WF.

where the water level $\mu = h_f^{(i)} + \frac{\Delta s}{\sum_{k \in E} w_k}$, as an isomorphism between μ and Δs , and (23) are utilized. When the working tunnel is escalated to the next pair of ceilings, $h_c^{(i)} = h_f^{(i+1)}$. It is seen that $V_{i+1}^{\min} = V_i^{\max}$, still based on the isomorphism between μ and Δs , and (23). Therefore, $\{g(\Delta s(\mu = h_f^{(i)}))\}$ is a monotonically increasing sequence in i tunnel, and thus Corollary 1 is proved. \square

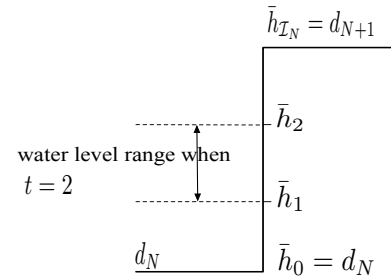


Fig. 6: Illustration of Step 2.2 of Algorithm GC-WF.

IV. EXTENDED EE MAXIMIZATION PROBLEM WITH THROUGHPUT REQUIREMENT

In this section, an extended EE maximization problem is further considered, by adding the requirement of minimum throughput B (unit: bits). The extended problem is formulated as

$$\begin{aligned} \max_{\{s_k\}_{k=1}^K} & \frac{\frac{1}{2} \sum_{k=1}^K w_k \log_2(1+a_k s_k)}{s_0 + \sum_{k=1}^K s_k} \\ \text{(EE-SIT)} \quad \text{s.t.} & \quad 0 \leq s_k \leq P_k, \text{ for } k = 1, \dots, K; \\ & \quad \sum_{k=1}^K s_k \leq P; \\ & \quad \frac{1}{2} \sum_{k=1}^K w_k \log_2(1 + a_k s_k) \geq B. \end{aligned} \quad (31)$$

As a side note, B cannot be too large for the existence of the solution. Since problem (31) requires $\frac{1}{2} \sum_{k=1}^K w_k \log_2(1 + a_k P_k) \geq B$, the P-GWFPP Algorithm is combined with Algorithm GC-WF to form a new algorithm for problem (31). The interesting fact is that P-GWFPP deletes the non-linear throughput constraint of problem (31), which can provide a substantial convenience to solve problem (31). More details can be found in the proof of Proposition 3.

A. Extended Algorithm GC-WFT

Algorithm GC-WFT:

0) Pre-process:

$$\begin{aligned} & \{E_f, k^*, \hat{P}(k^*)\} \\ & = \text{GWFP} \left(\{a_k, w_k, P_k\}_{k=1}^K, \min \left\{ \sum_{k=1}^K P_k, P \right\} \right) \\ & \text{and} \\ & a_{K+1} w_{K+1} = \left(\frac{\hat{P}(k^*)}{\sum_{k \in E_f} w_k} + \frac{1}{a_{k^*} w_{k^*}} \right)^{-1}. \end{aligned} \quad (32)$$

1) Implementing P-GWFPP, we have:

$$(\{s_k\}, k^*) = \text{P-GWFPP}(\{a_k, w_k, P_k\}_{k=1}^K, B). \quad (33)$$

2) Let $\mu_0 = \frac{s_{k^*}}{w_{k^*}} + d_{k^*}$. Determine $[d_N, d_{N+1}]$ and then the tunnel floor and ceiling $[h_f, h_c]$ such that $\mu_0 \in [h_f, h_c] \subset [d_N, d_{N+1}]$. Assign a $1 \times K$ vector $(S_{0,1}, \dots, S_{0,K}) = (s_1, \dots, s_K)$, where (s_1, \dots, s_K) has been obtained from Step 1).

3) Implement GC-WF, only changing the phrase in Step 3) of GC-WF:

$$n^* = \arg \max_{\{N|1 \leq N \leq K\}} \left\{ \frac{\frac{1}{2} \sum_{k=1}^K w_k \log_2(1+a_k S_{N,k})}{s_0 + \sum_{k=1}^K S_{N,k}} \right\}, \quad (34)$$

into

$$n^* = \arg \max_{\{N|0 \leq N \leq K\}} \left\{ \frac{\frac{1}{2} \sum_{k=1}^K w_k \log_2(1+a_k S_{N,k})}{s_0 + \sum_{k=1}^K S_{N,k}} \right\} \\ \left| \sum_{k=1}^K S_{N,k} \geq \sum_{k=1}^K s_k \right\}. \quad (35)$$

Then output $\bar{s}_k = S_{n^*,k}, \forall k$, as the solution.

The following proposition states optimality of GC-WFT.

Proposition 3. GC-WFT outputs the solution to (31) with a finite amount of computation.

Proof. Notice the P-GWFPP's providing the initial interval $[d_N, d_{N+1}]$ and its subinterval $[h_f, h_c]$ mentioned in 2) of GC-WFT. (31) is equivalent to

$$\begin{aligned} \max_{\{s_k\}_{k=1}^K} & \frac{\frac{1}{2} \sum_{k=1}^K w_k \log_2(1+a_k s_k)}{s_0 + \sum_{k=1}^K s_k} \\ \text{subject to} & \quad s_k \leq s_k \leq P_k, \text{ for } k = 1, \dots, K; \\ & \quad \sum_{k=1}^K s_k \leq \sum_{k=1}^K P_k, \end{aligned} \quad (36)$$

where $\{\underline{s}_k\}_{k=1}^K$ is the solution to the problem of

$$\begin{aligned} \min_{\{s_k\}_{k=1}^K} & \sum_{k=1}^K s_k \\ \text{subject to} & \quad 0 \leq s_k \leq P_k, \text{ for } k = 1, \dots, K; \\ & \quad \sum_{k=1}^K s_k \leq P; \\ & \quad \frac{1}{2} \sum_{k=1}^K w_k \log_2(1 + a_k s_k) \geq B. \end{aligned} \quad (37)$$

The proof of equivalence is as follows. Let $\{s_k^*\}_{k=1}^K$ be the optimal solution to (36). $\{s_k^*\}_{k=1}^K$ is a feasible solution to (31). Thus, the optimal objective value of (36) is no greater than that of (31). Substitute the optimal solution into (37), and the equality of the last constraint holds. Assume, to the contrary, that $\frac{1}{2} \sum_{k=1}^K w_k \log_2(1 + a_k \underline{s}_k) > B$, where $\{\underline{s}_k\}_{k=1}^K$ is an optimal solution to (37). Accordingly, we can use the less power to satisfy all the constraints of (37). Thus, the objective value in $\{\underline{s}_k\}_{k=1}^K$ is not minimal. The contradiction is obtained. Therefore, the equality can be taken. Similarly, the equality of the last constraint holds in for (1) with $E_0 = \{1, \dots, K\}$. Therefore, the optimal solution to (37) is unique. The detailed proof is as follows. Assume, to the contrary, that $\{s_k^*\}$ and $\{s_k^{**}\}$ are two different solutions to (37). Thus, the two achieved throughputs in $\{s_k^*\}$ and $\{s_k^{**}\}$ are equal to the same numerical value as B in (37). Since $\{s_k^*\}$ and $\{s_k^{**}\}$ have been assumed as the two different solutions to (37), $\sum_k s_k^*$ and $\sum_k s_k^{**}$ are the optimal values (refer to [18, p. 127]) of (37) and identical. If the P of the total power budget is assign by $\sum_k s_k^*$, (1) has optimal solutions of $\{s_k^*\}$ and $\{s_k^{**}\}$. Since the objective function of (1) has a negative-definite Hessian matrix and (1) has a convex feasible set, (1) only has a unique solution. Hence, $\{s_k^*\}$ and $\{s_k^{**}\}$ are identical. A contradiction is obtained. Therefore, the optimal solution to (37) is unique, although the objective function of (37) is not strictly convex. Then, a point is the solution to (37) if and only if the point is obtained through P-GWFPP. The insight is: no matter what method is used to solve (37), such a solution can always be obtained by implementing P-GWFPP.

Conversely, let $\{s_k^*\}_{k=1}^K$ be the optimal solution to (31). Thus, $\frac{1}{2} \sum_{k=1}^K w_k \log_2(1 + a_k s_k^*) \geq B$. It is seen that $\{s_k^*\}_{k=1}^K$ is the optimal solution to (37), where B is assigned by the value of $\frac{1}{2} \sum_{k=1}^K w_k \log_2(1 + a_k s_k^*)$. This updated B is labeled as B_1 , to differentiate from the original B , and $B_1 \geq B$. As a result, $\{s_k^*\}_{k=1}^K$ and $\{\underline{s}_k\}_{k=1}^K$ are the solutions to (37) with B_1 and B , respectively. Due to the assumed monotonicity of $\{a_k w_k\}$ in (9), k^* with the constraint of $\frac{1}{2} \sum_{k=1}^K w_k \log_2(1 + a_k s_k^*) = B_1$ is greater than that with the constraint of $\frac{1}{2} \sum_{k=1}^K w_k \log_2(1 + a_k \underline{s}_k) = B$. Else if k^* with the constraint of $\frac{1}{2} \sum_{k=1}^K w_k \log_2(1 + a_k s_k^*) = B_1$ is equal to that with the constraint of

$\frac{1}{2} \sum_{k=1}^K w_k \log_2(1 + a_k \underline{s}_k) = B$, $s_k^* \geq \underline{s}_k, \forall k$, according to (10). Thus, for the both cases above, we obtain that $\{s_k^* \geq \underline{s}_k\}_{k=1}^K$, and $\{s_k^*\}_{k=1}^K$ is a feasible point of (36). Therefore, the optimal objective value of (31) is not greater than that of (36). As (31) is not less than that of (36) either, the optimal objective value of (31) is equal to that of (36). Therefore, (31) and (36) have the same set of the optimal solutions. According to the formal definition of equivalence between optimization problems (refer to [28, Definition 3.3.1]), (31) and (36) are equivalent.

As a result, (36) does not have the constraint of $\frac{1}{2} \sum_{k=1}^K w_k \log_2(1 + a_k s_k) \geq B$. That is to say, P-GWFPP removes a non-linear constraint of coupling power in (31) under the mentioned equivalence. For (31), the optimality proof of GC-WFT only focuses on its equivalent (36). with referring to Appendix B (*i.e.*, the poof of Proposition 2). Therefore, optimality of GC-WFT is obtained. \square

Corollary 2. GC-WFT conducts iterative computation of Eq. (25) once at most.

Proof. Corollary 2 can be proved by a similar way of Corollary 1, and the proof is omitted here. \square

Remark 4. In [17], we provided an analogous comparison of the mechanism of the proposed approach with the well known Dinkelbach's method. The advantages were summarized into two points: search range and solving each convex optimization problem. In this paper, we extended the energy efficient maximization problem to include individual upper power bound constraints. With these additional constraints, the advantages of the proposed approach is more significant over Dinkelbach's method. The detail is mentioned below, and more details will also be presented in the Section V with numerical results analysis.

For this class of energy efficiency maximization problems, most existing algorithms, such as the widely adopted Dinkelbach's algorithm [29], need two levels of iteration loops: the inner (iteration) loop and the outer (iteration) loop. The inner loop aims to compute the point to satisfy certain conditions (eg., condition (B) referring to [29, p. 495]). The obtained point is usually an optimal solution to an auxiliary optimization problem instead of the target one. In addition, many of the inner loops are needed to generate a sequence, which is further utilized in the outer loop to find the optimal solution with convergence. However, in fact, such a sequence is difficult to obtain. Firstly, every point in the sequence requires a finite amount of computation to obtain the exact numerical value in the inner loop. Secondly, the convergence in the outer loop may breakdown, since the inner loop may fail to find the exact solution ([30]). Instead, our proposed algorithms converge to the exact solution with efficient computations.

V. COMPLEXITY ANALYSIS AND NUMERICAL RESULTS

A. Complexity Analysis

GC-WFT of problem (31) is a more general problem than GC-WF of problem (12), and owns a higher computational complexity. Thus, we focus on providing the computational complexity analysis on Algorithm GC-WFT.

Since GC-WFT utilizes GC-WF, which depends on Steps 2.X.1), 2.X.2) and 2.X.3). However, Step 2.X.3) is only utilized once at most, by GC-WF. Here, Step 2.X.3) includes $N_t (= N_1 + N_2)$ (defined in Appendix A) iterations to compute the solution, with the exactness, to (24). Given $\{d_N\}$ and the corresponding tunnel floor, $\{h_f\}$, it is seen that completing the N_t iterations needs $10K \max_{\{1 \leq i \leq 2K\}} \{\frac{h_c}{h_f} + 35\}$ basic arithmetic, logical, and elementary function evaluation operations at most, with the computational complexity level of $O(K)$ under the given P . At the same time, Steps 2.X.1) and 2.X.2) are only utilized $2K + 1$ evaluations of $g(\cdot)$ at most and in total, by GC-WFT. This is because the evaluations are determined by $\{d_N\}_{N=1}^{K+1}$ and $\{c_N\}_{N=1}^K$ and the sets of $\{d_N\}_{N=1}^{K+1}$ and $\{c_N\}_{N=1}^K$ have $2K + 1$ members together. As a side note, $g(\Delta s_{\max})$ for the given interval or subinterval is equal to $g(0)$ for the next interval or subinterval, where the index of the interval or the subinterval is not beyond $2K + 1$. These points are obtained from the definition of $g(\Delta s)$ (refer to (21) and (23)) and the statement of GC-WF. Furthermore, each of the $2K + 1$ evaluations of $g(0)$ s or $g(\Delta s_{\max})$ s over the intervals or the subintervals needs, at most, $4K - 1$ basic arithmetic operations; K basic elementary function evaluation operations where $\log(\cdot)$ in $g(\Delta s)$ is the assigned basic elementary function; and K basic assignment operations, $2K$ basic arithmetic operations and 1 basic logical operation (of material implication) that judges the positiveness of the $g(\cdot)$ for the power allocation in the statement of GC-WF. The (basic) operation means the four classes of basic operations above. Therefore, the number of the (basic) operations is not greater than $(2K + 1) \times (4K - 1 + 4K + 1) = 16K^2 + 8K$. Therefore, the $2K + 1$ evaluations of $g(\cdot)$ in total, by GC-WFT, may take any number greater than $16K^2 + 8K$, such as $36K^2 + 12K$, for an upper bound of the number for completing their operations. That is to say, computational complexity of the $2K + 1$ evaluations of $g(\cdot)$ in total, by GC-WFT, can be expressed into $O(K^2)$ by the big O notation [31].

Sorting $\{d_n, c_n\}$ needs the complexity of $O(K \log(K))$. Since GWFPP and P-GWFPP are utilized by GC-WFT, this utilization uses the computational complexity of $O(K^2)$ (refer to [27] and [12]). As a result, since $O(K) + O(K^2) + O(K \log(K)) + O(K^2) = O(K^2)$, GC-WFT has the computational complexity of $O(K^2)$.

On the other hand, one of the most efficient convex optimization algorithms is selected as PD-IPM, either for Dinkelbach's method using multiple times or for PD-IPM directly and independently being used as an algorithm. The computational complexity of PD-IPM, only being used once, is $O(K^{3.5}) \log(1/\epsilon)$ [18], [32]. Ours is to compute the

solution with the error of machine zero; while PD-IPM is to compute an ϵ solution.

Therefore, we have following proposition.

Proposition 4. For the proposed problems, GC-WFT outputs the exact optimal solution and the computational complexities of $O(K^2)$; while PD-IPM outputs an ϵ solution with the computational complexity of $O(K^{3.5}) \log(1/\epsilon)$.

B. Numerical Results

A numerical example is firstly presented in this subsection to illustrate the proposed algorithms. We could choose any other practical parameters for the target problems, because optimality and computational complexity of the proposed algorithms GC-WF and GC-WFT have already been proven, strictly. In addition, the performance of the proposed algorithms is compared with the Dinkelbach's algorithm with numerical results, as intuitive illustrations.

Example 1. Instantiating the weighted case of EE-PPT by GC-WFT, this problem is:

$$\begin{aligned} \max_{\{s_i\}_{i=1}^2} & \frac{\frac{2}{3} \log(1+s_1) + \log(1+0.5s_2)}{1+s_1+s_2} \\ \text{subject to: } & s_i \geq 0, \forall i; \\ & s_1 \leq 5, s_2 \leq 1; \\ & s_1 + s_2 \leq 3; \\ & \frac{2}{3} \log(1+s_1) + \log(1+0.5s_2) \geq \frac{\log 13.5}{3}. \end{aligned} \quad (38)$$

The solving procedures are listed in Table I.

TABLE I: Iteration results for Example 1

n	\mathbf{S}	Efficiency
0	$\begin{bmatrix} 1 & 1 \\ 0 & 0 \\ 0 & 0 \end{bmatrix}$	$\frac{\log(13.5)}{9} = 0.2892$ 0 0
1	$\begin{bmatrix} 1 & 1 \\ 1/3 & 0 \\ 0 & 0 \end{bmatrix}$	$\frac{\log(13.5)}{3} = 0.2892$ $\frac{\log(4/3)}{2} = 0.1438$ 0
2	$\begin{bmatrix} 1 & 1 \\ 1/3 & 0 \\ 1.2899 & 1 \end{bmatrix}$	0.2892 0.1438 0.2911
	[1.2899 1.0]	0.2911

According to Step 3) in GC-WFT, the case at $n = 1$ has been ruled out. At the same time, the case, with the first sub-interval $[h_f, h_c]$, at $n = 2$ has also been ruled out. It is seen that this example has the optimal solution (1.2899, 1) and the maximum efficiency of 0.2911.

A stochastic experiment is further conducted to validate the computational efficiency of the proposed algorithms. Since GC-WFT is more general, it is taken a representative of the proposed algorithms. The parameters $\{a_k, w_k\}$ are assigned at random, where the square root of each entry of $\{a_k\}$ is drawn independently from the standard Gaussian distribution and then squared (due to a_k being a channel power-gain, $\forall k$), and each entry of $\{w_k\}$ independently from a uniform distribution of $U[0, 1]$. Each of the experiments is conducted based on 100 samples, with both the sum power

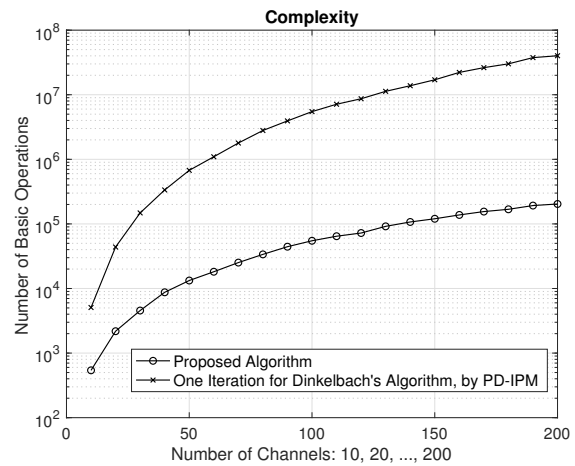


Fig. 7: Comparing computational complexity of GC-WFT with that of one iteration of Dinkelbach's algorithm.

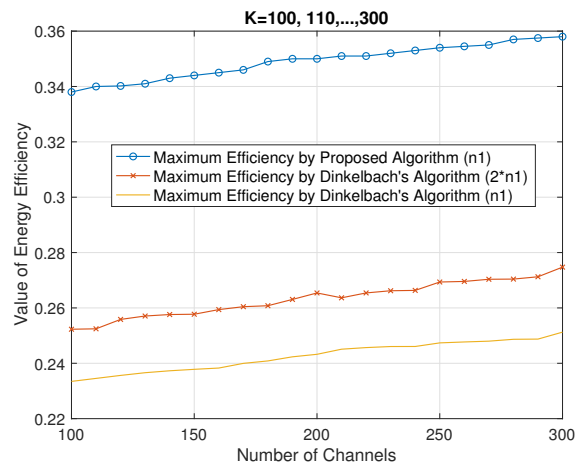


Fig. 8: Maximum energy efficiency by GC-WFT vs. Dinkelbach's algorithm (1).

bound being set up from 10 dBm to 200 dBm (*i.e.*, 1dBm times the number of the channels) and the peak power values being taken at $U[1, 1.5]$ with the unit of dBm. The computational complexity of the proposed GC-WFT is compared with that of the Dinkelbach's algorithms with $\epsilon = 0.01$, as shown in Fig. 7. The result demonstrates that the proposed GC-WFT requires much less computation, and this advantage becomes more significant as the number of channels increases.

Fig. 8 shows the EE performance of the proposed GC-WFT algorithm, where “n1” denotes the computation complexity (*i.e.*, the number of basic operations). In addition, the EE achieved by the Dinkelbach's algorithm at the same and double computation costs is also shown for comparison, labeled as “n1” and “2*n1”, respectively. Compared with the Dinkelbach's algorithm, the proposed GC-WFT algorithm can improve the system EE by around 35% while reducing the computational cost by 50%, revealing the efficiency of the proposed algorithm. The reason is that the Dinkelbach's

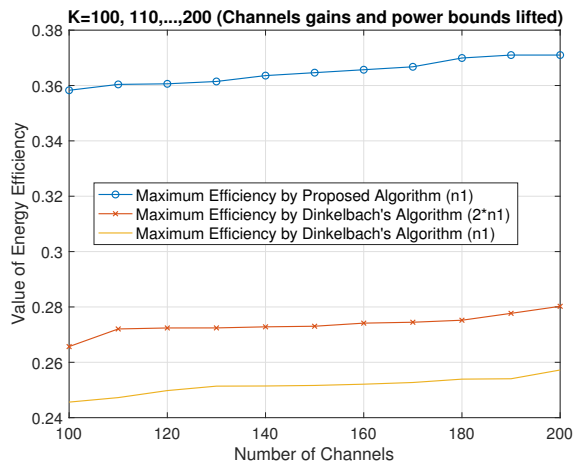


Fig. 9: Maximum energy efficiency by GC-WFT vs. Dinkelbach's algorithm (2).

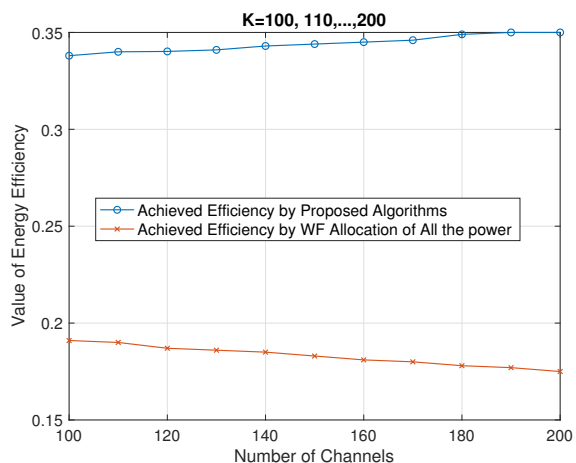


Fig. 10: Achieved energy efficiency by GC-WFT vs. achieved energy efficiency by WF allocating all the power.

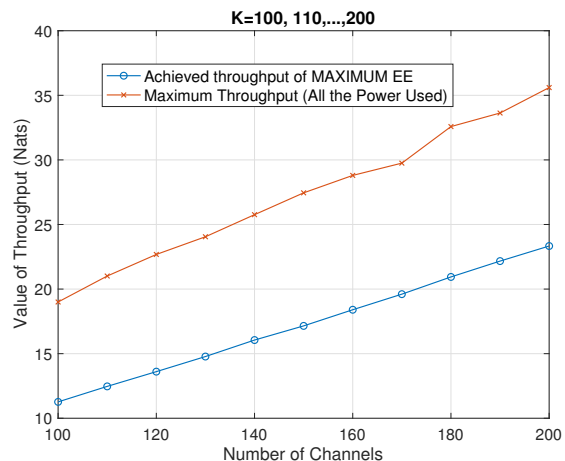


Fig. 11: Different Objective Function: throughput by GC-WFT vs. by WF.

algorithm is iterative and utilizes the line search (eg.,

PD-IPM), which leads to slow performance improvement. Furthermore, the proposed algorithms can be implemented through parallel computations. Therefore, GC-WFT can be applied to solve super-large-scale problems with high efficiency and exactness, such as the massive Multiple Input Multiple Output (MIMO) systems.

The performances of GC-WFT and Dinkelbach algorithms are also compared under different system parameters, as shown in Fig. 9. $\{a_k\}$ are increased by 10% to reflect different channel condition, the individual power bounds and sum power bound are lifted by 25% to denote different power budgets. Fig. 9 also shows similar results, validating the effectiveness of the proposed GC-WFT algorithm. As a side note, the EE does not increase linearly with the channel gain or power bounds, due to the form of the objective function in (12).

Fig. 10 shows the energy efficiency achieved by the proposed GC-WFT algorithms and the energy efficiency by water-filling to allocate all the available power when the number of channels, K , changes from 100 to 200. The proposed algorithm is shown to increase the energy efficiency by 83-116%, compared with the EE by solving the maximum throughput. The gain is more significant as the number of channels increases. At the same time, $\{g(\Delta s_{max})\}$ cannot be guaranteed to be non-positive. Thus, it is not always recommended to allocate out all the available power, for maximizing energy efficiency.

The important insight of Fig. 10 is that EE-optimal and throughput-optimal solutions may not be consistent. In fact, there exists a trade-off relationship between EE and throughput in practical systems. To demonstrate this trade-off relationship, we compare the throughput performance between the GC-WFT and conventional throughput-optimal water-filling power allocation algorithms, as shown in Fig. 11. The line marked with circles shows the throughput achieved by the GC-WFT algorithm, labeled as "Achieved throughput of MAXIMUM EE". The other line represents the maximum throughput in problem (1), labeled as "Maximum Throughput". Specifically, the cost to achieve EE-optimal is to sacrifice the system throughput by around 35-40%. For the implementation, the EE can be maximized while meeting the system throughput requirement, by adjusting the throughput threshold B in problem (EE-SIT) (31).

VI. CONCLUSION

We proposed an efficient power allocation algorithm to solve the generally weighted energy efficiency maximization problems with both the individual peak and whole power constraints, based on a geometric ceiled water tank illustration. Furthermore, the algorithm has also been extended to solve the problem with the additional minimum throughput requirement. The proposed algorithms guarantee optimality and the efficiency simultaneously. Numerical examples have been provided to demonstrate that the proposed algorithm can reduce the computational complexity

by more than two orders, or improve the energy efficiency by about 50% with the same amount of computations compared with the conventional Dinkelbach's method. Moreover, the proposed algorithms are with a parallel computation structure, and thus provide effective power allocation solutions to achieve the optimal energy-efficient large-scale system power allocation policies.

APPENDIX A PROOF OF PROPOSITION 1

For the i and the N involved in forming the problem (24), $g(\Delta s)$ is given in this system, where the parameter sets, $\{E, E^c\}$, of $g(\Delta s)$ depend on the i and the N . The derivative $g'(\Delta s)$ of $g(\Delta s)$ at $\Delta s = 0$ is

$$g'(0) = \frac{\sum_{k \in E} w_k \log \frac{h_i}{d_k} + \sum_{k \in E^c} w_k \log \frac{\mu_k}{d_k}}{\sum_{k \in E} w_k} \quad (39)$$

and then $g'(0) \geq 0$. At the same time,

$$g''(\Delta s) = \frac{1}{\Delta s + h_i \sum_{k \in E} w_k} > 0 \text{ for } \Delta s \in (0, \Delta s_{\max}). \quad (40)$$

Thus, $g'(\Delta s) > 0$ for $\Delta s \in (0, \Delta s_{\max})$, and it is strictly monotonically increasing in this domain of Δs . It is easy to see that case two and case three, as trivial cases, only need much less computation for evaluating $g(0)$ and $g(\Delta s_{\max})$ and have the corresponding conclusions in Proposition 1. Since $g(\Delta s)$ is strictly monotonically increasing, there is no case of $g(0) > 0$ and $g(\Delta s_{\max}) < 0$. Therefore, we only focus case one: $g(0) < 0$ and $g(\Delta s_{\max}) > 0$ to solve the system of $g(\Delta s) = 0$ and $\Delta s \in (0, \Delta s_{\max})$ or problem (24). Also it is true that uniqueness of the solution is guaranteed if this condition above holds.

The remaining part refers to the second paragraph in [17, Appendix B], which includes its (52).

Proposition 1 is hence proved.

APPENDIX B PROOF OF PROPOSITION 2

Since the objective function in (12) is continuous over the feasible set that is compact, it is seen that there exists an optimal solution to (12). Let $\{s_k^*\}_{k=1}^K$ denote an optimal solution to (12) under the meaning of global optimality.

The optimal solution of $\{s_k^*\}_{k=1}^K$ implies that it is also the solution to the following problem:

$$\begin{aligned} \max_{\{s_k\}_{k=1}^K} & \frac{1}{2} \sum_{k=1}^K w_k \log_2(1 + a_k s_k) \\ \text{subject to:} & 0 \leq s_k \leq P_k, \forall k; \\ & \sum_{k=1}^K s_k = \sum_{k=1}^K s_k^*. \end{aligned} \quad (41)$$

Successively, (41) and GWFPP (refer to its statement mentioned above) or the details in [27]) result in the facts that there exist $n \in \mathbb{Z}^+$ with $1 \leq n \leq K$ and then $[h_i, h_{i+1}]$ such that $\frac{s_k^*}{w_k} + \frac{1}{a_k w_k} \in [h_i, h_{i+1}], \forall k \in E$. Here, as a reminder, E depends on n and h_i . At the same time, $\frac{s_k^*}{w_k} + \frac{1}{a_k w_k}$ is constant, $\forall k \in E$. On the other hand,

$s_k^* = \left[(h_i - d_k) + \frac{s_k^*}{w_k} \right] w_k, \forall k \in E$; and $s_k^* = P_k, \forall k \in E^c$. Also, $s_k^* = 0, \forall k \in \{1, \dots, K\} \setminus (E \cup E^c)$. These facts may utilize the partitions of $\{d_n\}$ and $\{h_i\}$ mentioned in the definition of $g(\Delta s)$, with referring to those usages by item 2.1) or item 2.2) of GC-WF.

Then, it is seen that the optimal value $\frac{\frac{1}{2} \sum_{k=1}^K w_k \log_2(1 + a_k s_k^*)}{s_0 + \sum_{k=1}^K s_k^*}$ of (12) is not less than the optimal value of the problem:

$$\begin{aligned} \max_{\{s_k\}_{k=1}^K} & \frac{\frac{1}{2} \sum_{k=1}^K w_k \log_2(1 + a_k s_k)}{s_0 + \sum_{k=1}^K s_k} \\ \text{subject to:} & 0 \leq s_k \leq P_k, \forall k; \\ & \sum_{k=1}^K s_k = V_{n,i}, \end{aligned} \quad (42)$$

for any given $V_{n,i}$ where $V_{n,i} \in [\sum_{k \in E^c} P_k + \sum_{k \in E} (h_i - d_k) w_k, \sum_{k \in E^c} P_k + \sum_{k \in E} w_k (h_{i+1} - d_k)]$. An optimal solution to (42) is denoted by $\{\underline{s}_k\}$. Thus, there exists Δs with $0 \leq \Delta s \leq \Delta s_{\max}$ such that $\underline{s}_k = \left[(h_i - d_k) + \frac{\Delta s}{w_k} \right] w_k$, for $k \in E$; $\underline{s}_k = P_k$, for $k \in E^c$; and $\underline{s}_k = 0, \forall k \in \{1, \dots, K\} \setminus (E \cup E^c)$ if available. These cases stem from $\{\underline{s}_k\}$ also being the solution, through the water-filling of GWFPP, to problem (42) with its water level in $[h_i, h_{i+1}]$. Due to the mentioned relationship between the two optimal values of (12) and (42), we have:

$$\frac{\sum_{k=1}^K \log(1 + a_k s_k^*)}{s_0 + \sum_{k=1}^K s_k^*} \geq \frac{\sum_{k=1}^K \log(1 + a_k \underline{s}_k)}{s_0 + \sum_{k=1}^K \underline{s}_k}. \quad (43)$$

$\{s_k^*\}_{k=1}^K$ and $\{\underline{s}_k\}_{k=1}^K$ having the aforementioned water-filling forms, implies the following the maximization problem:

$$\begin{aligned} \max_{\Delta s} & \frac{\sum_{k \in E} w_k \log[1 + a_k (\mu - d_k) w_k] + \sum_{k \in E^c} w_k \log(1 + a_k P_k)}{s_0 + \sum_{k \in E} (\mu - d_k) w_k + \sum_{k \in E^c} P_k} \\ \text{subject to:} & \mu = h_i - d_k + \frac{\Delta s}{w_k}, \forall k \in E; \\ & 0 \leq \Delta s \leq \Delta s_{\max}, \end{aligned} \quad (44)$$

and interestingly, such an obtained optimization problem only has a single optimization variable. It is seen that the optimal solution to (44) is $\frac{s_k^*}{w_k} \times \sum_{k \in E} w_k$, denoted by Δs^* . Further, let us denote the objective function of (44) by $f(\Delta s)$. The derivative of $f(\Delta s)$, $f'(\Delta s)$, is expressed into:

$$f'(\Delta s) = \frac{1}{\mu [s_0 + \sum_{k \in E} (\mu - d_k) w_k + \sum_{k \in E^c} P_k]^2} \times \left\{ [s_0 + \sum_{k \in E} (\mu - d_k) w_k + \sum_{k \in E^c} P_k] - \mu \left[\sum_{k \in E} w_k \log \left(\frac{\mu}{d_k} \right) + \sum_{k \in E^c} w_k \log \left(\frac{\mu_k}{d_k} \right) \right] \right\}, \quad (45)$$

where $0 \leq \Delta s \leq \Delta s_{\max}$. As a reminder, it is seen that $\mu_k = d_k + \frac{P_k}{w_k}, k \in E^c$. Since the denominator part keeps the positive sign, the zero and the positive or negative signs of $f'(\Delta s)$ only depend on the essential numerator part of

$$\left\{ [s_0 + \sum_{k \in E} (\mu - d_k) w_k + \sum_{k \in E^c} P_k] - \mu \left[\sum_{k \in E} w_k \log \left(\frac{\mu}{d_k} \right) + \sum_{k \in E^c} w_k \log \left(\frac{\mu_k}{d_k} \right) \right] \right\}. \quad (46)$$

Thus, for convenience and simplification, the numerator part times “-1” is denoted by $g(\Delta s)$ which is the same as that defined in Proposition 1, based on the reference being selected by minimizing $-f(\Delta s)$. Of course, one may also choose the symmetric maximization of $f(\Delta s)$. As mentioned before, $g'(0) \geq 0, g'(\Delta s) \uparrow$, for $\Delta s \in [0, \Delta s_{\max}]$, and then $g''(\Delta s) > 0$, within valid range of Δs . Therefore,

- if $g(0) > 0$, $\Delta s^* = 0$ and then $s_k^* = (h_i - d_k)w_k = \underline{s}_k$, for $k \in E$; $s_k^* = P_k = \underline{s}_k$, for $k \in E^c$; while $s_k^* = 0 = \underline{s}_k$, for other k s if available;
- if $g(\Delta s_{\max}) < 0$, $\Delta s^* = \Delta s_{\max}$ and then $s_k^* = (h_{i+1} - d_k)w_k = \underline{s}_k$, for $k \in E$; $s_k^* = P_k = \underline{s}_k$, for $k \in E^c$; while $s_k^* = 0 = \underline{s}_k$, for other k s if available; and
- if $g(0) \cdot g(\Delta s_{\max}) < 0$, $\Delta s^* = AO(s_0, n, \{d_k\}, [h_i, h_{i+1}])$ and $s_k^* = (\frac{\Delta s^*}{\sum_{k \in E} w_k} + h_i - d_k)w_k = \underline{s}_k$, for $k \in E$; $s_k^* = P_k = \underline{s}_k$, for $k \in E^c$; while $s_k^* = 0 = \underline{s}_k$, for other k s if available.

As a result, the machine expression of $\{s_k^*\}$ is indeed identical to the output of GC-WF. From the aforementioned computational analysis, the practical exact solution is computed by a finite amount of computation.

Proposition 2 is hence proved.

REFERENCES

- [1] S. Lambert, W. Van Heddeghem, W. Vereecken, B. Lannoo, D. Colle, and M. Pickavet, "Worldwide electricity consumption of communication networks," *Optics express*, vol. 20, no. 26, pp. B513–B524, 2012.
- [2] "C-RAN: the road towards green RAN," Tech. Rep., China Mobile, 2011.
- [3] Y. Soh, T. Quek, M. Kountouris, and H. Shin, "Energy efficient heterogeneous cellular networks," *IEEE J. Select. Areas Commun.*, vol. 31, no. 5, pp. 840–850, 2013.
- [4] D. Feng, C. Jiang, G. Lim, L. Cimini, G. Feng, and G. Y. Li, "A survey of energy-efficient wireless communications," *IEEE Commun. Surveys Tut.*, vol. 15, no. 1, pp. 167–178, 2013.
- [5] J. G. Andrews, S. Buzzi, W. Choi, S. V. Hanly, A. Lozano, A. CK. Soong, and J. Z. Zhang, "What will 5G be?," *IEEE J. Select. Areas Commun.*, vol. 32, no. 6, pp. 1065–1082, 2014.
- [6] D. Tsilimantos, J. Gorce, K. Jaffrès-Runser, and H. V. Poor, "Spectral and energy efficiency trade-offs in cellular networks," *IEEE Trans. Wireless Communications*, vol. 15, no. 1, pp. 54–66, 2016.
- [7] Z. Hasan, H. Boostanimehr, and V. K. Bhargava, "Green cellular networks: A survey, some research issues and challenges," *IEEE Commun. Surveys Tut.*, vol. 13, no. 4, pp. 524–540, Nov. 2011.
- [8] M. Ismail, W. Zhuang, E. Serpedin, and K. Qaraqe, "A survey on green mobile networking: From the perspectives of network operators and mobile users," *IEEE Commun. Surveys Tut.*, vol. 17, no. 3, pp. 1535–1556, 2015.
- [9] V. Tsibonis, L. Georgiadis, and L. Tassiulas, "Exploiting wireless channel state information for throughput maximization," *IEEE Trans. Inform. Theory*, vol. 50, no. 11, pp. 2566–2582, 2004.
- [10] S. Ekbatani, F. Etemadi, and H. Jafarkhani, "Throughput maximization over slowly fading channels using quantized and erroneous feedback," *IEEE Trans. Communications*, vol. 57, no. 9, 2009.
- [11] L. P. Qian, Y. J. Zhang, and J. Huang, "Mapel: Achieving global optimality for a non-convex wireless power control problem," *IEEE Trans. Wireless Communications*, vol. 8, pp. 1553–1563, 2009.
- [12] P. He and L. Zhao, "Solving a class of sum power minimization problems using generalized water-filling," *IEEE Trans. Wireless Communications*, vol. 14, no. 12, pp. 6792–6804, 2015.
- [13] S. Zhang, J. Gong, S. Zhou, and Z. Niu, "How many small cells can be turned off via vertical offloading under a separation architecture?," *IEEE Trans. Wireless Communications*, vol. 14, no. 10, pp. 5440–5453, Oct 2015.
- [14] M. Ismail, A. T. Gamage, W. Zhuang, X. Shen, E. Serpedin, and K. Qaraqe, "Uplink decentralized joint bandwidth and power allocation for energy-efficient operation in a heterogeneous wireless medium," *IEEE Trans. Communications*, vol. 63, no. 4, pp. 1483–1495, 2015.
- [15] S. Kandukuri and S. Boyd, "Optimal power control in interference-limited fading wireless channels with outage-probability specifications," *IEEE Trans. Wireless Communications*, vol. 1, no. 1, pp. 46–55, 2002.
- [16] L. P. Qian, Y. Wu, H. Zhou, and X. Shen, "Joint uplink base station association and power control for small-cell networks with non-orthogonal multiple access," *IEEE Trans. Wireless Communications*, vol. 16, no. 8, pp. 5567–5582, Aug. 2017.

- [17] P. He, S. Zhang, L. Zhao, and X. Shen, "Multi-channel power allocation for maximizing energy efficiency in wireless networks," *IEEE Trans. Vehicular Tech.*, to appear.
- [18] S. Boyd and L. Vandenberghe, *Convex Optimization*, Cambridge University Press, Cambridge, 2004.
- [19] D. P. Bertsekas, *Nonlinear Programming, 2nd Edition*, Athena Scientific, Nashua, 1999.
- [20] M. Avriel, *Nonlinear Programming: Analysis and Methods*, Prentice-Hall, Inc., 1976.
- [21] Q. Wu, M. Tao, and W. Chen, "Joint Tx/Rx energy-efficient scheduling in multi-radio wireless networks: A divide-and-conquer approach," *IEEE Trans. Wireless Communications*, vol. 15, no. 4, pp. 2727–2740, 2016.
- [22] G. Ozcan, M. C. Gursoy, N. Tran, and J. Tang, "Energy-efficient power allocation in cognitive radio systems with imperfect spectrum sensing," *IEEE Journal on Selected Areas in Communications*, vol. 34, no. 12, pp. 3466–3481, 2016.
- [23] Q. Wu, W. Chen, M. Tao, J. Li, H. Tang, and J. Wu, "Resource allocation for joint transmitter and receiver energy efficiency maximization in downlink OFDMA systems," *IEEE Trans. Communications*, vol. 63, no. 2, pp. 416–430, 2015.
- [24] D. W. K. Ng, E. S. Lo, and R. Schober, "Energy-efficient resource allocation in OFDMA systems with large numbers of base station antennas," *IEEE Trans. Wireless Communications*, vol. 11, no. 9, pp. 3292–3304, 2012.
- [25] D. Zhang, Z. Chen, J. Ren, N. Zhang, M. Awad, H. Zhou, and X. Shen, "Energy harvesting-aided spectrum sensing and data transmission in heterogeneous cognitive radio sensor network," *IEEE Trans. Vehicular Tech.*, vol. PP, no. 99, pp. 1–1, 2016.
- [26] J. Ren, Y. Zhang, N. Zhang, D. Zhang, and X. Shen, "Dynamic channel access to improve energy efficiency in cognitive radio sensor networks," *IEEE Trans. Wireless Communications*, vol. 15, no. 5, pp. 3143–3156, 2016.
- [27] P. He, L. Zhao, S. Zhou, and Z. Niu, "Water-filling: A geometric approach and its application to solve generalized radio resource allocation problems," *IEEE Trans. Wireless Communications*, vol. 12, no. 7, pp. 3637–3647, 2013.
- [28] P. He and L. Zhao, "Optimal power allocation for maximum throughput of general mu-mimo multiple access channels with mixed constraints," *IEEE Trans. Communications*, vol. 64, no. 3, pp. 1042–1054, 2016.
- [29] W. Dinkelbach, "On nonlinear fractional programming," *Management Science*, vol. 13, no. 7, pp. 492–498, 1967.
- [30] W. Zangwill, *Nonlinear Programming: A Unified Approach*, Prentice-Hall, Englewood Cliffs, 1969.
- [31] C. H. Papadimitriou and K. Steiglitz, *Combinatorial Optimization: Algorithms and Complexity, Unabridged edition*, Dover Publications, Mineola, 1998.
- [32] L. Zhang, Y. Xin, Y.-C. Liang, and H. V. Poor, "Cognitive multiple access channels: Optimal power allocation for weighted sum rate maximization," *IEEE Trans. Communications*, vol. 57, pp. 2754–2762, 2009.



Peter He (S'15-M'15) received the M.A.Sc. degree in electrical engineering from McMaster University, Hamilton, ON, Canada, in 2009. He received the Ph.D. degree in electrical engineering from Ryerson University, Toronto, Canada, in 2015. His interests are the union of large-scale optimization, information theory, communications, and smart power grid. During his Ph.D. studies, he has been continuously awarded Graduate Research Excellence Award in Department of Electrical and Computer Engineering at Ryerson University and OGS (Ontario Graduate Scholarship) awards. He was awarded NSERC (Natural Sciences and Engineering Research Council) Postdoctoral Fellowship in 2016. He is a recipient of the Best Paper Award of the 2013 International Conference on Wireless Communications and Signal Processing (WCSP).



Shan Zhang (S'13-M'16) received her Ph.D. degree in electronic engineering from Tsinghua University, Beijing, China, in 2016. She is currently an assistant professor in the School of Computer Science and Engineering, Beihang University, Beijing, China. She was a post doctoral fellow in Department of Electronical and Computer Engineering, University of Waterloo, Ontario, Canada, from 2016 to 2017. Her research interests include mobile edge computing, wireless network virtualization and intelligent management. Dr.

Zhang received the Best Paper Award at the Asia-Pacific Conference on Communication in 2013.



Xuemin (Sherman) Shen (M'97-SM'02-F'09) received the Ph.D. degree in electrical engineering from Rutgers University, New Brunswick, NJ, USA, in 1990. He is currently a University Professor with the Department of Electrical and Computer Engineering, University of Waterloo, Waterloo, ON, Canada. His research focuses on resource management in interconnected wireless/wired networks, wireless network security, social networks, smart grid, and vehicular ad hoc and sensor networks. He is a registered

Professional Engineer of Ontario, Canada, an Engineering Institute of Canada Fellow, a Canadian Academy of Engineering Fellow, a Royal Society of Canada Fellow, and a Distinguished Lecturer of the IEEE Vehicular Technology Society and Communications Society.

Dr. Shen received the Joseph LoCicero Award in 2015 and the Education Award in 2017 from the IEEE Communications Society. He has also received the Excellent Graduate Supervision Award in 2006 and the Outstanding Performance Award 5 times from the University of Waterloo, and the Premiers Research Excellence Award (PREA) in 2003 from the Province of Ontario, Canada. He served as the Technical Program Committee Chair/Co-Chair for the IEEE Globecom16, the IEEE Infocom14, the IEEE VTC10 Fall, the IEEE Globecom07, the Symposia Chair for the IEEE ICC10, the Tutorial Chair for the IEEE VTC11 Spring, the Chair for the IEEE Communications Society Technical Committee on Wireless Communications, and P2P Communications and Networking. He is an Editor-in-Chief of the IEEE INTERNET OF THINGS JOURNAL and the Vice President on publications of the IEEE Communications Society.



Lian Zhao (S'99-M'03-SM'06) received the Ph.D. degree from the Department of Electrical and Computer Engineering (ELCE), University of Waterloo, Canada, in 2002. She joined the Department of Electrical and Computer Engineering at Ryerson University, Toronto, Canada, in 2003 and a Professor in 2014. Her research interests are in the areas of wireless communications, radio resource management, power control, cognitive radio and cooperative communications, optimization for complicated

systems.

She received the Best Land Transportation Paper Award from IEEE Vehicular Technology Society in 2016; Top 15 Editor in 2015 for IEEE Transaction on Vehicular Technology; Best Paper Award from the 2013 International Conference on Wireless Communications and Signal Processing (WCSP) and Best Student Paper Award (with her student) from Chinacom in 2011; the Ryerson Faculty Merit Award in 2005 and 2007; the Canada Foundation for Innovation (CFI) New Opportunity Research Award in 2005, and Early Tenure and promotion to Associate Professor in 2006. She has been an Editor for IEEE TRANSACTION ON VEHICULAR TECHNOLOGY since 2013; co-chair for IEEE ICC 2018 Wireless Communication Symposium; workshop co-chair for IEEE/CIC ICC 2015; local arrangement co-chair for IEEE VTC Fall 2017 and IEEE Infocom 2014; co-chair for IEEE Global Communications Conference (GLOBECOM) 2013 Communication Theory Symposium. She served as a committee member for NSERC (Natural Science and Engineering Research Council of Canada) Discovery Grants Evaluation Group for Electrical and Computer Engineering 2015-2018. She is a licensed Professional Engineer in the Province of Ontario, a senior member of the IEEE Communication and Vehicular Society.